Physica B 173 (1991) 99–111
North-Holland

Invited paper

Reflection theory and the analysis of neutron reflection data

John Lekner
Department of Physics, Victoria University, Wellington, New Zealand

A unified formulation of reflection theory is given in a form which may be applied to neutron or electromagnetic wave reflection. Some exact results are given, valid for an arbitrary stratification, and then approximations based on these are developed, and compared. Matrix and numerical methods of calculating reflectivities are also discussed. Finally, an old problem, concerning the existence of a thin layer of water on ice below 0°C, is suggested as one which may be resolved by means of neutron reflection studies.

1. Introduction

All reflection, whether of particle, electromagnetic or acoustic waves, is the result of the constructive interference of many scattered waves originating from scatterers in a planar stratified medium. For regular arrays (gratings or lattices), specular reflection can be viewed as a special case of diffraction: it is the zeroth order diffraction peak, and the *only* one when the wavelength is greater than twice the lattice spacing. When the latter condition holds, an assembly of scatterers can be replaced by a medium characterized by an effective potential V, or dielectric function ε, or refractive index n.

For planar-stratified media whose properties depend spatially only on the depth z, reflection properties follow (in principle, at least) from the knowledge of $V(z)$ or $\varepsilon(z)$ or $n(z)$. Fermi and others [1–5] demonstrate that for neutrons with scattering length b off (bound) scatterers occupying volume v per scatterer, the effective potential or refractive index are given by

$$V = \left(\frac{\hbar^2}{2m}\right) 4\pi b/v\ , \qquad n^2 = 1 - \lambda^2 b/\pi\ . \tag{1}$$

The one-to-one correspondence between reflection of electromagnetic s-waves and particle waves is well known [5, 6]. For the study of reflection properties it is convenient to deal in terms of an effective dielectric function $\varepsilon = n^2$, which from (1) is

$$\varepsilon = 1 - \lambda^2/L^2\ , \qquad L^2 \equiv \pi v/b\ . \tag{2}$$

The dielectric function for electromagnetic waves in an electron gas or plasma,

$$\varepsilon = 1 - \omega_p^2/\omega^2\ , \tag{3}$$

has the same form as (2), with $L^2 = \pi v/r_e$, where v is the volume per electron and $r_e = e^2/mc^2 \approx 2.818 \times 10^{-15}$ m is the classical electron radius. It is interesting that the formula for L is so similar in the two cases, with b and r_e both of nuclear size. The same form for ε holds for X-rays away from atomic resonance frequencies. Although the form taken by the effective dielectric function is the same, the volume per scatterer can be very different. We note also that L can be imaginary for neutrons, for

0921-4526/91/$03.50 © 1991 – Elsevier Science Publishers B.V. (North-Holland)

scatterers with a negative scattering length, as for example protons, or lithium 7. (Reflection experiments are however always done on media with positive b and L^2, since these media have $\varepsilon < 1$ and thus can reflect strongly.) The magnitudes of v and L are shown in table 1 for some typical cases.

At a boundary between two media with dielectric functions ε_1 and ε_2, Snell's law reads

$$\varepsilon_1 \cos^2\theta_1 = \varepsilon_2 \cos^2\theta_2 \,, \tag{4}$$

where θ_1 and θ_2 are the (glancing) angles of incidence and refraction. For incidence from the vacuum, where $\varepsilon_1 = 1$, and with $\varepsilon_2 = 1 - \lambda^2/L_2^2$, reflection is total (a real θ_2 ceases to exist) for

$$\sin\theta_1 \leq \sin\theta_c = \lambda/\mathrm{L}_2 \tag{5}$$

Thus radio waves with $\lambda/\sin\theta_1 > L_2$ will reflect back down to earth from the ionosphere, or sodium will strongly reflect electromagnetic waves at normal incidence for $\lambda > 2090$ Å. (The reflection is not complete in either of these examples; absorption has been omitted from (3)). For thermal neutrons the wavelengths are typically much shorter than the length L, and very small glancing angles of incidence are used in order to work near enough to the equality in (5) to obtain sufficient reflected flux.

In the remainder of this paper we will concentrate on neutron reflection, and will present some general results of reflection theory in the special context of particle reflection at near grazing incidence. We consider a general stratification where $L^2(z) = \pi v(z)/b(z) = \pi/\rho(z)$ varies with depth z ($\rho = b/v$ is the scattering length density). The resulting effective dielectric function is

$$\varepsilon(z) = 1 - \lambda^2/L^2(z) = 1 - \lambda^2\rho(z)/\pi \,, \tag{6}$$

and for particle or electromagnetic s-waves the reflection problem is characterized by a one-dimensional wave equation (for proofs see for example sections 1-1 and 1-3 of ref. [5]),

$$\frac{d^2\psi}{dz^2} + q^2(z)\psi = 0 \,, \tag{7}$$

where the full probability amplitude for plane wave propagation in the zx plane is $\Psi(z,x) = \psi(z)\exp(iKx)$, and K and q are the components of the propagation vector along and perpendicular to the stratification. K is an invariant, obtained mathematically as a separation of variables constant, and its constancy implies Snell's law (4), since $K = \sqrt{\varepsilon_1}(2\pi/\lambda)\cos\theta_1 = \sqrt{\varepsilon_2}(2\pi/\lambda)\cos\theta_2$, where ε_1 and ε_2 are the limiting values of $\varepsilon(z)$ above the inhomogeneity, which typically is confined to some thickness Δz. We normally have $\varepsilon_1 = 1$ (the neutrons are incident from a vacuum or a good approximation to it); in that case the perpendicular component of the propagation vector is given by

$$q^2(z) = \left(\frac{2\pi}{\lambda}\right)^2 [\varepsilon(z) - \cos^2\theta_1] = \left(\frac{2\pi}{\lambda}\right)^2 [\sin^2\theta_1 - \lambda^2/L^2(z)] \,, \tag{8}$$

Table 1

wave type	medium	volume per scatterer (Å^3)	L (Å)
thermal neutrons	niobium metal	18.0	981
X-rays	water	3.0	580
light	sodium metal	37.7	2090
radio waves	ionosphere	$\sim 10^{19}$	~100 m

or by

$$q^2(z) = q_1^2 - 4\pi b(z)/v(z) = q_1^2 - 4\pi\rho(z)\,, \tag{9}$$

with $q_1 = (2\pi/\lambda)\sin\theta_1$.

Total reflection, $|r| = 1$, occurs when q_2 is imaginary, which from (8) or (5) is when $\sin\theta_1 \leqslant \lambda/L_2$ (this result holds for all non-absorbing stratifications which are bounded above and below by a uniform media characterized by $\varepsilon_1 = 1$ and ε_2, as we shall see shortly). From (8) we have $q_2 = (2\pi/\lambda)(\varepsilon_2 - \cos^2\theta_1)^{1/2}$, imaginary when $\theta_1 \leqslant \theta_c = \arccos\sqrt{\varepsilon_2} = \arcsin(\lambda/L_2)$ or $\lambda \geqslant \lambda_c = L_2\sin\theta_1$. When $b > 0$, so θ_c exists, we can write

$$q^2(z) = \left(\frac{2\pi}{L_2}\right)^2\left[\frac{\sin^2\theta_1}{\sin^2\theta_c} - \left(\frac{L_2}{L(z)}\right)^2\right] = 4\pi\left[\rho_2\frac{\sin^2\theta_1}{\sin^2\theta_c} - \rho(z)\right]. \tag{10}$$

Thus for fixed profile $\rho(z)$, the wave equation is the same for same values of $\sin\theta_1/\sin\theta_c = q_1/q_c$, where $q_c = (2\pi/\lambda)\sin\theta_c = 2\pi/L_2$.

The limiting forms of ψ define the reflection and transmission amplitudes r and t:

$$e^{iq_1z} + r\,e^{-iq_1z} \leftarrow \psi \rightarrow t\,e^{iq_2z}\,. \tag{11}$$

For unit incident flux, the reflected flux is $R = |r|^2$. Conservation of particles (or of electromagnetic energy) in the absence of absorption reads $R + T = 1$, where $T = (q_2/q_1)|t|^2$ (see section 2-1 of ref. [5].

An important special case is that of reflection at a step (a sharp interface between media 1 and 2). Taking the boundary at $z = 0$, and using the continuity of ψ and $d\psi/dz$ at the interface, gives

$$r_{\text{step}} = \frac{q_1 - q_2}{q_1 + q_2}\,, \qquad t_{\text{step}} = \frac{2q_1}{q_1 + q_2}\,. \tag{12}$$

The step reflection amplitude can be rewritten in terms of θ_c:

$$r_{\text{step}} = \frac{\sin\theta_1 - [\sin^2\theta_1 - \sin^2\theta_c]^{1/2}}{\sin\theta_1 + [\sin^2\theta_1 - \sin^2\theta_c]^{1/2}}\,. \tag{13}$$

There is a $(\theta_1 - \theta_c)^{1/2}$ singularity at the critical angle, corresponding to the right-angle turn which q_2 takes in the complex plane on passing through zero, and $R_{\text{step}} = |r_{\text{step}}|^2$ decreases rapidly from unity as θ_1 increases beyond θ_c: at $\sin\theta_1 = 2\sin\theta_c$ the reflectivity is $(2-\sqrt{3})^4 \approx 5\times10^{-3}$, while at normal incidence $R_{\text{step}} = (1-\cos\theta_c)/(1+\cos\theta_c) \approx (\lambda/2L_2)^4$, usually an undetectably small value for neutrons. (The approximate equality is valid when $\lambda \ll L_2$; for $\lambda \geqslant L_2$ the reflection is total at all angles.)

2. Some exact results for a general stratification

Two of the properties noted above for the step profile, namely that reflection is total for $\sin\theta_1 < \lambda/L_2$, and that the fall-off from total reflection occurs with a square-root singularity in $\theta_1 - \theta_c$, are common to all non-absorbing stratifications. We will consider a non-uniform bounded layer which may have discontinuities in $\rho(z)$, as shown in fig. 1.

For a given known variation of $\varepsilon(z)$ in the interval $[a, b]$, the second order differential equation (7) has two independent solutions, say $F(z)$ and $G(z)$. Thus $\psi(z)$ may be written as

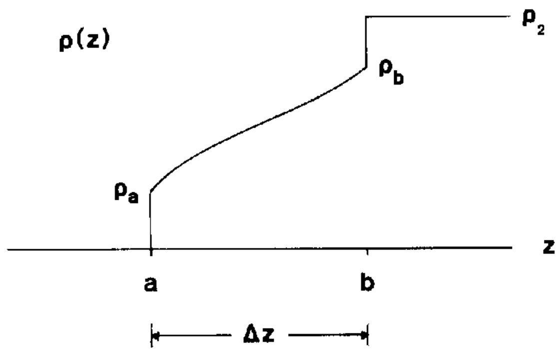

Fig. 1. Scattering length density profile, $\rho(z) = b(z)/v(z)$, for neutron reflection from a non-uniform layer. The variation between $z = a$ and $z = b$ may take arbitrary form.

$$\psi(z) = \begin{cases} e^{iq_1 z} + r\,e^{-iq_1 z}\,, & z < a\,, \\ \alpha F(z) + \beta G(z)\,, & a < z < b\,, \\ t\,e^{iq_2 z}\,, & z > b\,. \end{cases} \tag{14}$$

By matching ψ and $d\psi/dz$ at $z = a$ and b, the four unknown constants r, α, β, t may be solved for. The result for r is (cf. eq. (2.25) of ref. [5]

$$r = e^{2iq_1 a}\,\frac{q_1 q_2(F, G) + iq_1(F, G') + iq_2(F', G) - (F', G')}{q_1 q_2(F, G) + iq_1(F, G') - iq_2(F', G) + (F', G')}\,, \tag{15}$$

where

$$(F, G) \equiv F_a G_b - G_a F_b\,, \qquad (F, G') \equiv F_a G'_b - G_a F'_b\,, \qquad \text{etc.} \tag{16}$$

Here F_a stands for $F(z)$ evaluated at $z = a$, F'_a for the derivative of F evaluated at $z = a$, and so on. When ε is discontinuous at $z = a$ or b, the values and derivatives are to be understood as limits $z \to a^+$ and $z \to b^-$.

In the absence of absorption F and G may be taken to be real, since they are solutions of a linear differential equation with real coefficients. For $\sin\theta_1 < \lambda/L_2$, q_2 is imaginary and r takes the form $e^{2iq_1 a}(-f + ig)/(f + ig)$, with real f and g. Thus $|r| = 1$ and reflection is total.

At $\theta_c = \arcsin(\lambda/L_2)$, q_2 is zero. For θ_1 just a bit greater than θ_c (or equivalently, for λ just a bit shorter than $\lambda_c = L_2 \sin\theta_1$), q_2 is small, and expansion of (15) in powers of q_2 gives the reflectance decreasing from unity as

$$R = 1 - \frac{4q_1 q_2 W^2}{q_1^2(F, G')^2 + (F', G')^2} + O(q_2^2)\,, \tag{17}$$

where the Wronskian $W \equiv FG' - GF'$ is independent of z, and we have used the identity

$$(F, G)(F', G') - (F, G')(F', G) = W_a W_b = W^2\,. \tag{18}$$

Equation (17) demonstrates that the $(\theta_1 - \theta_c)^{1/2}$ singularity is universal for reflectivity as θ_1 tends to θ_c from above, since

$$q_2 = \frac{2\pi}{\lambda}\,[\sin^2\theta_1 - \sin^2\theta_c]^{1/2} \rightarrow \frac{2\pi}{\lambda}\,(\sin 2\theta_c)^{1/2}(\theta_1 - \theta_c)^{1/2}\,. \tag{19}$$

Equivalently, in terms of $\lambda_c = L_2 \sin\theta_1$, we have from (8) that

$$q_2 = \frac{2\pi}{\lambda L_2}\,[\lambda_c^2 - \lambda^2]^{1/2} \rightarrow \frac{2\pi}{L_2}\left(\frac{2}{\lambda_c}\right)^{1/2}(\lambda_c - \lambda)^{1/2}\,, \tag{20}$$

so there is a $(\lambda_c - \lambda)^{1/2}$ singularity in the wavelength variation as λ tends to $\lambda_c = L_2 \sin\theta_1$ from below.

The universality shown in (17) is a rigorous result for profiles of finite range (see ref. [24] for the case of profiles with $z^{-\mu}$ tail) but its range of validity may be very small in some special cases, as we shall see in section 5. Surface roughness or a spread of angles of incidence or of wavelengths will in any case smooth out the singularity near θ_c or λ_c (see for example fig. 3 of ref. [7] or fig. 2 of ref. [19]).

At grazing incidence ($\theta_1 \rightarrow 0$), $r \rightarrow -1$, as can be seen directly from (15). Thus all profiles reflect perfectly in the limit of grazing incidence (it is not necessary for ε_2 to be less than ε_1 for this to hold). On the other hand, as $\varepsilon_2 \rightarrow \varepsilon_1$, the reflection goes to zero: there has to be a change in the medium for reflection to occur. Since $\Delta\varepsilon$ is small for neutrons, reflection experiments are forced to operate near grazing incidence. Some difficulty is to be expected in theory which tries to deal with phenomena in a region of conflicting limits: here with $R \rightarrow 1$ at grazing incidence, $R \rightarrow 0$ as $\Delta\varepsilon \rightarrow 0$.

Among the many other exact and general results of reflection theory [5], we will omit all but two: the first is the exact expression (5.83) of ref. [5],

$$r = -\int_{-\infty}^{\infty} \mathrm{d}z\,\frac{\mathrm{d}q/\mathrm{d}z}{2q}\,(\mathrm{e}^{2\mathrm{i}\phi} - r^2(z)\,\mathrm{e}^{-2\mathrm{i}\phi})\,, \tag{21}$$

where $r(z)$ is the reflection amplitude of a profile truncated at z (profile truncation is illustrated in fig. 5-1 of ref. [5]), and $\phi(z)$ is the accumulated phase at z:

$$\phi(z) = \int^{z} \mathrm{d}\zeta\, q(\zeta)\,. \tag{22}$$

The second is the theorem that monotonic profiles reflect less than the step profile (proved in section 5-4 of ref. [5]), illustrated in fig. 2.

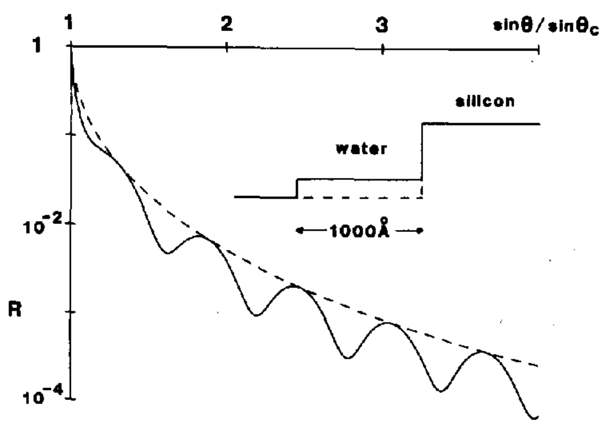

Fig. 2. Reflectivity of a layer of H_2O ($\rho = 0.056 \times 10^{-5}$ Å^{-2}) on Si ($\rho = 0.215 \times 10^{-5}$ Å^{-2}), compared to the reflection from bare Si, using (24) and (11). The water layer is 1000 Å thick.

3. Approximations based on the exact results

The expression (15) is exact, but usually we do not know the wave functions $F(z)$ and $G(z)$. When we do, as for the exponential, Rayleigh, or linear profiles (Sections 2-5 and 5-2 of ref. [5]), direct substitution in (15) gives the exact reflection amplitude. The simplest non-trivial case is that of a uniform profile, in which $q(z)$ is a constant q, and F and G may be taken as $\cos qz$ and $\sin qz$. This gives the familiar results (e.g. ref. [5], eqs. (2.52), (2.58))

$$r = \mathrm{e}^{2\mathrm{i}q_1 a}\,\frac{r_1 + r_2\,\mathrm{e}^{2\mathrm{i}q\,\Delta z}}{1 + r_1 r_2\,\mathrm{e}^{2\mathrm{i}q\,\Delta z}} = \mathrm{e}^{2\mathrm{i}q_1 a}\,\frac{q(q_1 - q_2)c + \mathrm{i}(q^2 - q_1q_2)s}{q(q_1 + q_2)c - \mathrm{i}(q^2 + q_1q_2)s}\,, \tag{23}$$

where $\Delta z = b - a$, $r_1 = (q_1 - q)/(q_1 + q)$ and $r_2 = (q - q_2)/(q + q_2)$ are the step or Fresnel reflection amplitudes at the boundaries of the uniform layer, $c = \cos q\,\Delta z$ and $s = \sin q\,\Delta z$. When q_1, q and q_2 are all real, the reflectivity is given by

$$R = |r|^2 = \frac{r_1^2 + 2r_1r_2\cos 2q\,\Delta z + (r_2)^2}{1 + 2r_1r_2\cos 2q\,\Delta z + (r_1r_2)^2}\,. \tag{24}$$

We seek approximations that remain exact in the special case of constant q, but allow for variation in $q(z)$ as in the profile of fig. 1. There is a sequence of such approximations, based on Liouville–Green waveforms (see section 6-2 of ref. [5]; in the physics literature these are usually referred to as WKB or JWKB wave functions). The zeroth order waveforms are $\cos\phi(z)$ and $\sin\phi(z)$. Using these we find

$$\begin{aligned} &(F, G) = \sin\Delta\phi\,, \qquad (F, G') = q_b\cos\Delta\phi\,, \\ &(F', G) = -q_a\cos\Delta\phi\,, \qquad (F', G') = q_aq_b\sin\Delta\phi\,, \end{aligned} \tag{25}$$

where $\Delta\phi$ is the total phase increment across the stratification:

$$\Delta\phi = \phi(b) - \phi(a) = \int_a^b \mathrm{d}z\; q(z)\,. \tag{26}$$

The values (25) substituted into (15) give, writing c for $\cos\Delta\phi$ and s for $\sin\Delta\phi$,

$$r_0 = \mathrm{e}^{2\mathrm{i}q_1 a}\,\frac{(q_1q_b - q_2q_a)c + \mathrm{i}(q_aq_b - q_1q_2)s}{(q_1q_b + q_2q_a)c - \mathrm{i}(q_aq_b + q_1q_2)s} \equiv \mathrm{e}^{2\mathrm{i}q_1 a}\,\frac{N_0}{D_0}\,. \tag{27}$$

When $q_a = q_b$, (27) reduces to the uniform layer reflection amplitude (23), and when $q_2 = 0$ (at the critical angle or critical wavelength), (27) correctly has unit modulus. Note that the extrema of $R_0 = |r_0|^2$ occur when $\Delta\phi$ is a multiple of $\frac{1}{2}\pi$.

The next approximation for the wave functions, namely

$$F(z) = \left(\frac{q_a}{q}\right)^{1/2}\cos\phi(z)\,, \qquad G(z) = \left(\frac{q_b}{q}\right)^{1/2}\sin\phi(z)\,, \tag{28}$$

(the square roots of q_a and q_b are inserted to give closer correspondence with our zeroth results) give

$$(F, G) = \sin \Delta\phi\ , \qquad (F, G') = q_b[\cos \Delta\phi - \tfrac{1}{2}\gamma_b \sin \Delta\phi]\ , \qquad (F', G) = -q_a[\cos \Delta\phi + \tfrac{1}{2}\gamma_a \sin \Delta\phi]\ ,$$
$$(F', G') = q_a q_b[\sin \Delta\phi + \tfrac{1}{2}(\gamma_b - \gamma_a) \cos \Delta\phi + \tfrac{1}{4}\gamma_a\gamma_b \sin \Delta\phi]\ , \tag{29}$$

where γ_a and γ_b are the values at $z = a^+$ and b^- of the dimensionless function extensively used in chapter 6 of ref. [5],

$$\gamma = \frac{\mathrm{d}q/\mathrm{d}z}{q^2} = -\frac{2\pi}{q^3}\frac{\mathrm{d}}{\mathrm{d}z}\left(\frac{b}{v}\right) = \frac{4\pi^2}{(qL)^3}\frac{\mathrm{d}L}{\mathrm{d}z}\ . \tag{30}$$

The values (29) substituted into (15) give the first order approximation to the reflection amplitude,

$$r_1 = \mathrm{e}^{2\mathrm{i}q_1 a}\,\frac{N_0 + N_1}{D_0 + D_1}\ , \tag{31}$$

where N_0 and D_0 are defined in (27), and

$$N_1 = -\tfrac{1}{2}(q_1 q_b \gamma_b + q_2 q_a \gamma_a)s + \frac{\mathrm{i}}{2}\, q_a q_b[(\gamma_b - \gamma_a)c + \tfrac{1}{2}\gamma_a\gamma_b s]\ ,$$
$$D_1 = -\tfrac{1}{2}(q_1 q_b \gamma_b - q_2 q_a \gamma_a)s - \frac{\mathrm{i}}{2}\, q_a q_b[(\gamma_b - \gamma_a)c + \tfrac{1}{2}\gamma_a\gamma_b s]\ . \tag{32}$$

Equation (31), like (27), gives the correct result for a uniform layer, and for an arbitrary layer it gives unit reflectivity at the critical angle or critical wavelength (when $q_2 = 0$).

According to the formulae for r_0 and r_1, reflection is mainly the result of discontinuities at $z = a$ and b, and of interference between the reflections from these discontinuities. Discontinuities in slope also contribute to r_1, while a gradual variation of the medium enters the formulae only through the phase increment $\Delta\phi$.

Another approximation scheme uses the exact relation (21) as starting point. If any truncation of the stratification can be expected to reflect weakly, then the term containing $r^2(z)$ in the integrand may be dropped. What results is called the Rayleigh, or weak reflection approximation [5]

$$r_\mathrm{R} = -\int_{-\infty}^{\infty} \mathrm{d}z\,\frac{\mathrm{d}q/\mathrm{d}z}{2q}\,\mathrm{e}^{2\mathrm{i}\phi}\ . \tag{33}$$

This works extremely well for smooth profiles which reflect weakly (see for example figs. 5-4 and 6-3 of ref. [5]). Further simplifications are possible, though the justification for these is mostly mathematical convenience: we can replace $2q(z)$ in the integrand by $q_1 + q_2$ (or $2q_1$, or $2q_2$) and $2\phi(z)$ by $(q_1 + q_2)z$. Then the modified Rayleigh approximation gives the reflection amplitude as a Fourier transform of $\mathrm{d}q/\mathrm{d}z$:

$$r'_\mathrm{R} = -\frac{1}{q_1 + q_2}\int_{-\infty}^{\infty} \mathrm{d}z\,\frac{\mathrm{d}q}{\mathrm{d}z}\,\mathrm{e}^{\mathrm{i}(q_1+q_2)z}\ , \tag{34}$$

(cf. eq. (1.109) and the related references and discussion in ref. [5]). Equation (34) has the virtues of simplicity, symmetry, and of giving the correct reflection amplitude for a step profile (for which $\mathrm{d}q/\mathrm{d}z = (q_2 - q_1)\delta(z)$ if the step is at the $z = 0$ plane, giving $r'_\mathrm{R} = (q_1 - q_2)/(q_1 + q_2) \equiv r_\mathrm{step}$). A slight modification of (34) is more convenient for neutron reflection. From $q^2(z) = q_1^2 - 4\pi b/v$, $dq/dz = -(2\pi/q)(d\rho/dz)$ where $\rho = b/v$ is the scattering length density. If we replace $q(z)$ by $1/2(q_1 + q_2)$ again, the resulting approximation is

$$r_R'' = \frac{4\pi}{(q_1 + q_2)^2} \int_{-\infty}^{\infty} dz \frac{d\rho}{dz} e^{i(q_1+q_2)z} . \tag{35}$$

This form can be modified to eq. (2.23) reported by Penfold and Thomas [7] and credited to Crowley [8], if $q_1 + q_2$ is replaced by $2q_1 \equiv \kappa$ ($h\kappa$ is the momentum transfer in the reflection process):

$$r_C = \frac{4\pi}{\kappa^2} \int_{-\infty}^{\infty} dz \frac{d\rho}{dz} e^{i\kappa z} . \tag{36}$$

How well do these various approximations work? We have already mentioned the special case of a step profile, for which (34) gives the correct answer, as do (27) and (31). For the uniform layer (or arbitrary thickness) only (27) and (31) give the correct answer. More important is the performance of these formulae when faced with a discontinuous and non-uniform profile, such as shown in fig. 1. We will compare (27), (31) and (36), using a linear variation in $\rho = b/v$. Then $q^2 = q_1^2 - 4\pi b/v$ is also linear in z, and the wave equation (6) is exactly solvable in terms of Airy functions [5]: the functions F and G in the formula (15) are given by $F(z) = A\mathrm{i}(-\zeta)$, $G(z) = B\mathrm{i}(-\zeta)$, where

$$\zeta(z) = \left(\frac{1}{4\pi}\left|\frac{\Delta z}{\Delta \rho}\right|\right)^{2/3} q^2(z) \equiv \left|\frac{\Delta z}{\Delta q^2}\right|^{2/3} q^2(z) , \tag{37}$$

with $\Delta\rho = \rho_b - \rho_a$ being the change in $\rho = b/v$ over the extent Δz of the profile.

For the approximate expressions (27) and (31) we need $\Delta\phi$, the increment in phase over the profile from $z = a$ to $z = b = a + \Delta z$. This is

$$\Delta\phi = \int_a^b dz\, q(z) = \frac{1}{6\pi} \frac{\Delta z}{\Delta\rho} (q_a^3 - q_b^3) . \tag{38}$$

For (31) we also need γ_a and γ_b, which from (30) are given by

$$\gamma_a = -2\pi \frac{\Delta\rho}{\Delta z} q_a^{-3} , \qquad \gamma_b = -2\pi \frac{\Delta\rho}{\Delta z} q_b^{-3} . \tag{39}$$

Finally, for the linear profile, the expression (36) gives (note that usually $\rho_1 = 0$)

$$r_C = \frac{4\pi}{\kappa^2} e^{i\kappa a}\left\{\rho_a - \rho_1 + (\rho_2 - \rho_b) e^{i\kappa \Delta z} + \frac{\Delta\rho}{\Delta z} (e^{i\kappa \Delta z} - 1)/i\kappa\right\} . \tag{40}$$

The reflectivities R_0, R_1 and R_C, obtained by squaring the modulus of (27), (32) and (36), are compared with the exact reflectivity in figs. 3 and 4. We see that R_0 is qualitatively correct, R_1 is accurate enough for most purposes, but that the simplifying approximations leading to (36) have thrown away too much information in the case of profiles with discontinuities. (For smooth, weakly reflecting profiles and away from θ_c the Rayleigh approximation works well, as has been noted above, and (36) can be obtained from r_R of eq. (33) by the steps outlined.)

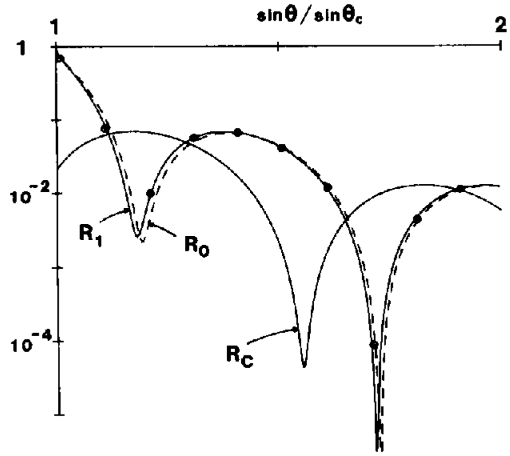

Fig. 3. Comparison of three approximate reflectivities for a profile with discontinuities in ρ at its boundaries, and a linear variation in $\rho(z)$ in between. The scattering length densities are $\rho_a = 0.641$, $\rho_b = 0.215$, $\rho_2 = 0.805$ (units of 10^{-5} Å^{-2}), and the layer thickness of 500 Å. R_0, R_1 and R_C are obtained from eqs. (27), (31) and (36). The circled points are exact values of R.

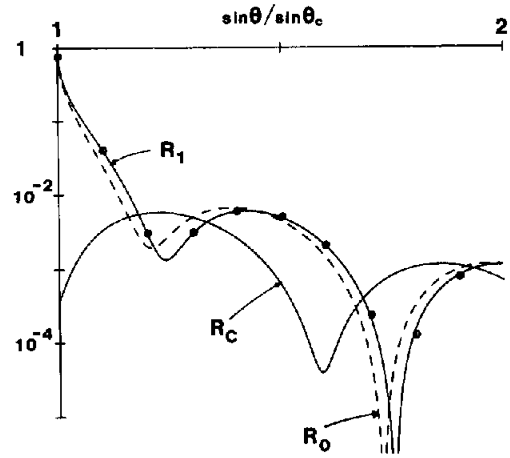

Fig. 4. As for fig. 3, with ρ_a and ρ_b intercanged: $\rho_a = 0.215$, $\rho_b = 0.641$, $\rho_2 = 0.805$ (units of 10^{-5} Å^{-2}). Note that R_0 is not as good as fig. 3, since less of the reflection is due to the (now smaller) discontinuities in ρ at the boundaries.

4. Matrix and numerical methods

The usual optical matrix method as given in Born and Wolf [9] has the unfortunate property of unnecessarily having imaginary off-diagonal matrix elements (in the absence of absorption). A minor change of starting point [5] gives real matrix elements, thus making the required matrix multiplication four times faster. Further improvements are possible, giving faster computation times for given accuracy [5, 10, 11]. We will outline these methods here.

The second order differential equation (6) is equivalent to two coupled first order equations (dependent variables ψ and ψ'):

$$\frac{\mathrm{d}}{\mathrm{d}z}\psi' + q^2\psi = 0\,, \qquad \psi' = \frac{\mathrm{d}\psi}{\mathrm{d}z}\,. \tag{41}$$

When $q(z)$ is approximated by a stack of N uniform layers, with value q_n in $z_n < z < z_{n+1}$ ($n = 1, \ldots, N$), we have in the nth layer

$$\begin{aligned} \psi(z) &= \psi_n \cos q_n(z - z_n) + q_n^{-1}\psi_n' \sin q_n(z - z_n)\,, \\ \psi'(z) &= \psi_n' \cos q_n(z - z_n) - q_n\psi_n \sin q_n(z - z_n)\,. \end{aligned} \tag{42}$$

(That the eqs. (41) are satisfied, and that $\psi(z_n) = \psi_n$, $\psi'(z_n) = \psi_n'$ can be seen directly from (42).) From (6) or (41) it follows that ψ and ψ' are continuous at discontinuities in q^2; continuity at z_{n+1} gives

$$\begin{aligned} \psi_{n+1} &= \psi_n \cos\delta_n + q_n^{-1}\psi_n' \sin\delta_n\,, \\ \psi_{n+1}' &= \psi_n' \cos\delta_n - q_n\psi_n \sin\delta_n\,, \end{aligned} \tag{43}$$

where $\delta_n = q_n(z_{n+1} - z_n) \equiv q_n\, \delta z_n$ is the phase increment across the nth layer. This pair of equations is conveniently written in matrix form,

$$\begin{pmatrix} \psi_{n+1} \\ \psi'_{n+1} \end{pmatrix} = \begin{pmatrix} \cos\delta_n & q_n^{-1}\sin\delta_n \\ -q_n\sin\delta_n & \cos\delta_n \end{pmatrix} \begin{pmatrix} \psi_n \\ \psi'_n \end{pmatrix} \equiv M_n \begin{pmatrix} \psi_n \\ \psi'_n \end{pmatrix} . \tag{44}$$

For the N layers we have

$$\begin{pmatrix} \psi_{N+1} \\ \psi'_{N+1} \end{pmatrix} = M_N M_{N-1} \ldots M_n \ldots M_2 M_1 \begin{pmatrix} \psi_1 \\ \psi'_1 \end{pmatrix} \equiv M \begin{pmatrix} \psi_1 \\ \psi'_1 \end{pmatrix} , \tag{45}$$

and thus the connection between the wave forms in the bounding (uniform) media is via the four matrix elements m_{ij} of the 2×2 profile matrix M, which is a product of the N layer matrices. Using the wave forms in (14), we find from (45) that the reflection amplitude is given by

$$r = e^{2iq_1z_1} \frac{q_1q_2m_{12} + iq_1m_{22} - iq_2m_{11} + m_{21}}{q_1q_2m_{12} + iq_1m_{22} + iq_2m_{11} - m_{21}} \tag{46}$$

(z_1 is equivalent to the a of the previous sections). Note the close correspondence with (15).

Numerically it is easy to take the product of 2×2 matrices, but the matrices M_n contain trigonometric functions, which are slow to evaluate. In addition, a given profile is better approximated by a stack of layers in which $q^2(z)$ or $\rho(z)$ varies linearly, for example

$$\rho(z) = \rho_n + (z - z_n)\, \delta\rho_n/\delta z_n \quad \text{in } z_n < z < z_{n+1} , \tag{47}$$

where $\delta\rho_n = \rho_{n+1} - \rho_n$. It is possible to incorporate the change in ρ over one layer, and avoid evaluation of the trig functions. For example, to third order in the dimensionless parameter $\delta_n = q_n\, \delta z_n$, and using the linear fit (47) gives [10]

$$\begin{pmatrix} 1 - \frac{1}{6}(2q_n^2 + q_{n+1}^2)(\delta z_n)^2 & \delta z_n - \frac{1}{12}(q_n^2 + q_{n+1}^2)(\delta z_n)^3 \\ -\frac{1}{2}(q_n^2 + q_{n+1}^2)\,\delta z_n + \frac{1}{30}(q_n^4 + 3q_n^2q_{n-1}^2 + q_{n+1}^4)(\delta z_n)^3 & 1 - \frac{1}{6}(q_n^2 + 2q_{n+1}^2)(\delta z_n)^2 \end{pmatrix} . \tag{48}$$

The matrix defined in (48) has determinant equal to unity plus a term of order $(q_n\, \delta z_n)^4$. The matrix defined in (44) has unit determinant (is unimodular). It turns out that unimodularity is necessary for two important conservation laws, particle conservation and reciprocity. The acoustic analogs are energy conservation and reciprocity; these are discussed in ref. [11], where it is shown how unimodular matrices may be constructed to represent any variation of $q(z)$ or $\rho(z)$ within a given layer. The second order unimodular matrix has the form

$$M_n = \begin{pmatrix} \dfrac{1 - I_2/2}{1 + I_2/2} & \dfrac{I_1}{1 + I_2/2} \\ \dfrac{-J_1}{1 + J_2/2} & \dfrac{1 - J_2/2}{1 + J_2/2} \end{pmatrix} , \tag{49}$$

where the relation $I_1J_1 = I_2 + J_2$ is guaranteed by the formalism. For linear variation in $\rho(z)$ or $q^2(z)$ within a given layer,

$$I_1 = \delta z_n, \quad J_1 = \tfrac{1}{2}(q_n^2 + q_{n+1}^2)\,\delta z_n,$$
$$I_2 = \tfrac{1}{6}(2q_n^2 + q_{n+1}^2)(\delta z_n)^2, \quad J_2 = \tfrac{1}{6}(q_n^2 + 2q_{n+1}^2)(\delta z_n)^2. \tag{50}$$

All the numerical matrix methods require $\delta_n = q_n\,\delta z_n$ to be small for accuracy (unless $q(z)$ is constant within a given region, in which case that region can be exactly represented by a matrix of the form given in (44)). Of the three methods discussed here, the third order, linear fit matrix (48) seems to be the most efficient in computation time for given accuracy.

5. Surface melting: is there a layer of water on ice below 0°C?

Many surface phenomena have been successfully explored by neutron reflection. Notable examples are the studies in surface physical chemistry by Thomas and collaborators [7, 12–15], and studies in surface magnetic properties by Felcher and collaborators [16–19]. Here we outline a long-standing problem to which neutron reflection could well make a decisive contribution, namely that of surface melting or premelting: the existence of a layer of liquid on solids below their bulk melting temperature T_m. The question of whether surface melting exists may be asked about any solid–liquid transition, and surface melting is part of the larger field of the wetting [20] of solid surfaces by liquids (not necessarily by the melt liquid). Here we will concentrate on the premelting of ice, which has great geophysical importance (compaction of snow, frost heaving, rock fracture, water transport at subzero temperatures, and charge transfer in ice-hail collisions in the electrification of thunder clouds are some of the related phenomena). Dash [21] gives a recent review of surface melting; the references go back to Faraday and to early ideas about the slipperyness of ice and about regelation (sintering).

Beaglehole and Nason [22] have found by ellipsometry that there is a large difference between premelting on the basal and the prismatic faces of ice crystals. On the basal face there appears to be premelting only very close of 0°C, while on the prismatic face there is a detectable layer down to about −7°C. At −1°C it is about 170 Å thick, with a rapid increase as 0°C is approached. A more recent ellipsometric experiment [23] verified that there is a liquid layer (with refractive index 1.33 for light of $\lambda = 6328$ Å) on both the basal and prismatic faces, but the detail of the temperature dependence was quite different to that of ref. [22]. The interpretation of the ellipsometric experiments is further complicated by the anisotropy of ice.

If neutron reflection experiments are done, it is likely that D_2O will be used. From ref. [4], $b(H_2O) = 1.68$ fm, $b(D_2O) = 19.14$ fm, so the relevant parameters for H_2O (near 0°C) and D_2O (near 3.81°C) are as shown in table 2. Figure 5 shows the expected reflectivities for a 500 Å layer of water on ice, and heavy water on heavy ice (the layers are assumed to be uniform). Since water is more dense than ice, there is a region near θ_c (or near λ_c) where q is imaginary. In this region the reflectivity is given by (using the second part of (23))

Table 2

	v (Å^3)	ρ (Å^{-2})	L (Å)
water	29.91	0.056×10^{-5}	2365
heavy water	30.08	0.636×10^{-5}	703
ice	32.62	0.0515×10^{-5}	2470
heavy ice[a]	32.81	0.583×10^{-5}	734

[a] The volume per molecule in heavy ice has been estimated by proportion.

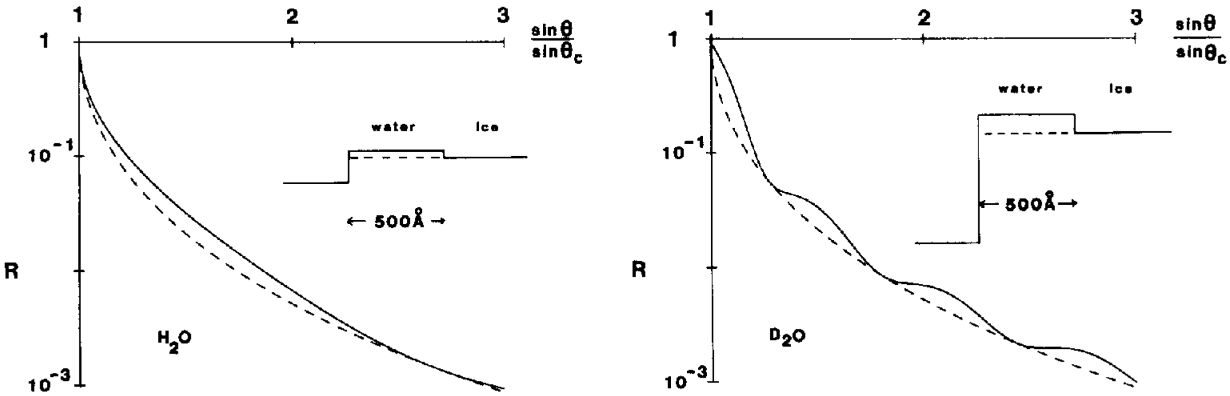

Fig. 5. Reflectivities due to a 500 Å thick layer of water on ice, shown for H_2O and D_2O. The dashed curve is the reflectivity due to ice alone, in both cases. The qualitative behaviour of the scattering length density is shown exaggerated: the actual change is only 9%.

$$R = \frac{|q|^2(q_1 - q_2)^2 + (q_1 q_2 + |q|^2)t^2}{|q|^2(q_1 + q_2)^2 + (q_1 q_2 - |q|^2)t^2}\,, \tag{51}$$

where $t = \tanh |q|\,\Delta z$. This has the limiting form

$$R = 1 - \frac{4q_1 q_2}{q_1^2 \cosh^2|q|\,\Delta z + |q|^2 \sinh^2|q|\,\Delta z} + \mathrm{O}(q_2^2)\,, \tag{52}$$

in accord with the general result obtained in section 2. But we noted there that the domain of validity of this $(\theta_1 - \theta_c)^{1/2}$ or $(\lambda_c - \lambda)^{1/2}$ singularity can be very small. From (51) we see that (52) is valid when $q_2 \ll q_1$ and $q_2 \ll |q|^2/q_1$. (The second condition is not required when $|q|\,\Delta z \ll 1$.) These conditions are satisfied when

$$\frac{\theta_1 - \theta_c}{\theta_c} \ll \tfrac{1}{2}\,, \qquad \frac{\theta_1 - \theta_c}{\theta_c} \ll \tfrac{1}{2}\left(\frac{\rho}{\rho_2} - 1\right)^2,$$

respectively. In the water–ice case, the second quantity is about 4×10^{-3}, and so the range of validity of (52) is restricted to extremely close to θ_c or λ_c, unless the water layer is so thin that $|q|\,\Delta z$ is small when θ_1 is near θ_c, which amounts to $\Delta z \ll [4\pi(\rho - \rho_2)]^{-1/2}$. This length is about 390 Å for D_2O and about 1330 Å for H_2O. These magnitudes explain the different behaviour near θ_c of the reflectivity for D_2O and H_2O with the same 500 Å thickness of liquid in each case, as shown in fig. 5.

Although the difference that a layer of water makes to the reflectivity is detectable if the layer is thick enough, precise temperature control, and preparation of crystals of ice with a sufficiently smooth and large reflecting face are likely to be difficult. Premelting of other solids may be easier to study by neutron reflection.

References

[1] E. Fermi, Nuclear Physics (University of Chicago Press, 1950) p. 201.
[2] D.J. Hughes, Neutron Optics (Wiley–Interscience, New York, 1954) p. 21.

[3] G.E. Bacon, Neutron Diffraction (Oxford University Press, Oxford, 1962) p. 116.
[4] A.G. Klein and S.A. Werner, Rep. Prog. Phys. 46 (1983) 259.
[5] J. Lekner, Theory of Reflection (Nijhoff/Kluwer, 1987) p. 17.
[6] M.L. Goldberger and F. Seitz, Phys. Rev. 71 (1947) 294.
[7] J. Penfold and R.K. Thomas, J. Phys. Cond. Mat. 2 (1990) 1369.
[8] T.L. Crowley, D. Phil Thesis, Oxford University (1984).
[9] M. Born and E. Wolf, Principles of Optics, 3rd Ed. (Pergamon, Oxford, 1965) Section 1.6.2.
[10] J. Lekner and M.C. Dorf, J. Opt. Soc. Am. 4 (1987) 2092.
[11] J. Lekner, J. Acoust. Soc. Am. 87 (1990) 2319.
[12] J.E. Bradley, E.M. Lee, R.K. Thomas, A.J. Willatt, J. Penfold, R.C. Ward, D.P. Gregory and W. Waschkowski, Langmuir 4 (1988) 821.
[13] E.M. Lee, R.K. Thomas, J. Penfold and R.C. Ward, J. Phys. Chem. 93 (1989) 381.
[14] J. Penfold, E.M. Lee and R.K. Thomas, Mol. Phys. 68 (1989) 33.
[15] A.R. Rennie, R.J. Crawford, E.M. Lee, R.K. Thomas, T.L. Crowley, S. Roberts, M.S. Qureshi and R.W. Richards, Macromolecules 22 (1989) 3466.
[16] G.P. Felcher, R.T. Kampwirth, K.E. Gray and R. Felici, Phys. Rev. Lett. 52 (1984) 1539.
[17] S.S.P. Parkin, R. Sigsbee, R. Felici and G.P. Felcher, Appl. Phys. Lett. 48 (1986) 604.
[18] G.P. Felcher, K.E. Gray, R.T. Kampwirth and M.B. Brodsky, Physica B 136 (1986) 59.
[19] A. Mansour, R.O. Hilleke, G.P. Felcher, R.B. Laibowitz, P. Chaudhari and S.S.P. Parkin, Physica B 156 & 157 (1989) 867.
[20] S. Dietrich, in: Phase Transitions and Critical Phenomena, eds. C. Domb and J. Lebowitz, Vol. 12 (1988).
[21] J.G. Dash, Contemp. Phys. 30 (1989) 89.
[22] D. Beaglehole and D. Nason, Surf. Sci. 96 (1980) 357.
[23] Y. Furakawa, M. Yamamoto and T. Kuroda, J. Crystal Growth 82 (1987) 665.
[24] S. Dietrich and R. Schack, Phys. Rev. Lett. 58 (1987) 140.